

divergence times for the Jamaican lineage. To determine the non-Jamaican rate, we used the mean genetic distance ($d = 0.036$) of two *Sesarma* species group comparisons. In each comparison, the genetic distance was determined for species on either side of the Isthmus of Panama. For the *reticulatum* group, this was *S. rhizophorae* versus *S. reticulatum*, *S. curacaoense*, and *S. sp.* (nr. *reticulatum*), $d = 0.031$ (16S rRNA, 0.020; COI, 0.041). For the *sulcatum* group, this was *S. crassipes* versus *S. sulcatum* and *S. aequatoriale*; $d = 0.042$ (16S rRNA, 0.021; COI, 0.062). These trans-isthmian species of intertidal and supratidal crabs presumably have not been isolated for more than 3.1 Myr (refs 19, 20). The resulting average rate of pairwise sequence divergence (which equals the non-Jamaican rate) was 1.17% per Myr (0.65% for 16S rRNA and 1.66% for COI, if analysed separately).

The mean genetic distance between the Jamaican lineage and the *reticulatum* group is 0.063 ± 0.005 (s.e.m.). A relative rate test²⁸ revealed a distance of 0.037 on the Jamaican lineage and 0.026 on the *reticulatum* group lineage. The time of divergence between the two lineages (4.54 ± 0.42 Myr) was estimated on the *reticulatum* group lineage by applying the non-Jamaican rate; the standard error of the divergence times is the standard error of the mean genetic distance divided by this rate. That time estimate (4.54 Myr), in turn, was used to calibrate the rate of pairwise sequence divergence within the Jamaican lineage (1.63% per Myr; 0.88% for 16S rRNA and 2.33% for COI) and estimate divergence times among species (Fig. 2) from the length of internal branches in Fig. 1. A nearly identical time estimate (4.56 Myr) for the origin of the Jamaican lineage was obtained if a gamma correction¹⁸ ($\alpha = 1.5$) was used to account for rate variation among sites. In two other decapod crustacean studies, estimated rates of pairwise sequence divergence for these two genes were higher: 2.2% per Myr for 16S rRNA in hermit crabs²¹ and 2.2–2.6% per Myr for COI in snapping shrimps²². Although the rate calibrated within *Sesarma* is preferred, application of those independent rates would result in an even more recent time estimate (2.4–2.9 Myr ago) for the origin of the Jamaican lineage.

Received 10 November 1997; accepted 2 March 1998.

- Hartnoll, R. G. in *Biology of the Land Crabs* (eds Burgegren, W. W. & McMahon, B. R.) 6–54 (Cambridge Univ. Press, Cambridge, 1988).
- Diesel, R. Parental care in an unusual environment: *Metopaulias depressus* (Decapoda: Grapsidae), a crab that lives in epiphytic bromeliads. *Anim. Behav.* **38**, 561–575 (1989).
- Diesel, R. Maternal control of calcium concentration in the larval nursery of the bromeliad crab, *Metopaulias depressus* (Grapsidae). *Proc. R. Soc. Lond. B* **264**, 1403–1406 (1997).
- Diesel, R. & Schuh, M. Maternal care in the bromeliad crab, *Metopaulias depressus* (Decapoda): maintaining oxygen, pH and calcium levels optimal for the larvae. *Behav. Ecol. Sociobiol.* **32**, 11–15 (1993).
- Diesel, R. Maternal care in the bromeliad crab, *Metopaulias depressus*: protection of larvae from predation by damselfly nymphs. *Anim. Behav.* **43**, 803–812 (1992).
- Diesel, R. & Horst, D. Breeding in a snail shell: ecology and biology of the Jamaican montane crab *Sesarma jarvisi* (Decapoda: Grapsidae). *J. Crust. Biol.* **15**, 179–195 (1995).
- Hedges, S. B. & Burnell, K. L. The Jamaican radiation of *Anolis* (Sauria: Iguanidae): an analysis of relationships and biogeography using sequential electrophoresis. *Carib. J. Sci.* **26**, 31–44 (1990).
- Hedges, S. B. An island radiation: allozyme evolution in Jamaican frogs of the genus *Eleutherodactylus* (Leptodactylidae). *Carib. J. Sci.* **25**, 123–147 (1989).
- Hass, C. A. & Hedges, S. B. Albumin evolution in West Indian frogs of the genus *Eleutherodactylus* (Leptodactylidae): Caribbean biogeography and a calibration of the albumin immunological clock. *J. Zool.* **225**, 413–426 (1991).
- Hedges, S. B. Historical biogeography of West Indian vertebrates. *Annu. Rev. Ecol. Syst.* **27**, 163–196 (1996).
- Hartnoll, R. G. The freshwater grapsid crabs of Jamaica. *Proc. Linn. Soc. Lond.* **175**, 145–169 (1964).
- Schubart, C. D., Reimer, J., Diesel, R. & Türkay, M. Taxonomy and ecology of two endemic freshwater crabs from western Jamaica with the description of a new *Sesarma* species (Brachyura: Grapsidae: Sesarminae). *J. Nat. Hist.* **31**, 403–419 (1997).
- Hartnoll, R. G. *Sesarma cookei* n. sp., a grapsid crab from Jamaica (Decapoda, Brachyura). *Crustaceana* **20**, 257–262 (1971).
- Sérène, R. & Soh, C. L. New Indo-Pacific genera allied to *Sesarma* Say 1817 (Brachyura, Decapoda, Crustacea). *Treubia* **27**, 387–416 (1970).
- Holthuis, L. B. in *Stygofauna Mundi* (ed. Botosaneanu, L.) 589–615 (Leiden, 1986).
- Guinot, D. in *Encyclopédie Biospéologique* (eds Jubertine, C. & Decou, V.) 165–179 (Société de Biospéologie, Moulis et Bucarest, 1994).
- Swofford, D. L. *Phylogenetic Analysis using Parsimony (PAUP)* (Univ. Illinois, Champaign, 1993).
- Kumar, S., Tamura, K. & Nei, M. *MEGA: Molecular Evolutionary Genetics Analysis* (Pennsylvania State Univ., University Park, 1993).
- Keigwin, L. Isotopic paleoceanography of the Caribbean and East Pacific: role of Panama uplift in late neogene time. *Science* **217**, 350–353 (1982).
- Coates, A. G. et al. Closure of the Isthmus of Panama: the near-shore marine record of Costa Rica and western Panama. *Geol. Soc. Am. Bull.* **104**, 814–828 (1992).
- Cunningham, C. W., Blackstone, N. W. & Buss, L. W. Evolution of king crabs from hermit crab ancestors. *Nature* **355**, 539–542 (1992).
- Knowlton, N., Wright, L. A., Solórzano, L. A., Mills, D. K. & Bermingham, E. Divergence in proteins, mitochondrial DNA, and reproductive compatibility across the Isthmus of Panama. *Science* **260**, 1629–1632 (1993).
- Carroll, R. L. Revealing the patterns of macroevolution. *Nature* **381**, 19–20 (1996).
- Brusca, R. C. & Brusca, G. J. *Invertebrates* (Sinauer, Sunderland, MA, 1990).
- Abele, L. G. A review of the grapsid crab genus *Sesarma* (Crustacea: Decapoda: Grapsidae) in America, with the description of a new genus. *Smithson. Contrib. Zool.* **527**, 1–60 (1992).

- Haq, B. U., Hardenbol, J. & Vail, P. R. Chronology of fluctuating sea levels since the Triassic. *Science* **235**, 1156–1167 (1987).
- Williamson, M. *Island Populations* (Oxford Univ. Press, Oxford, 1981).
- Palumbi, S. R. et al. *The Simple Fool's Guide to PCR. A Collection of PCR Protocols* (University of Hawaii, Honolulu, 1991).
- Cabot, E. L. & Beckenbach, A. T. Simultaneous editing of multiple nucleic acid and protein sequences with ESEE. *Comp. Appl. Biosci.* **5**, 233–234 (1989).
- Takezaki, N., Rzhetsky, A. & Nei, M. Phylogenetic test of the molecular clock and linearized trees. *Mol. Biol. Evol.* **12**, 823–833 (1995).

Acknowledgements. We thank P. K. L. Ng, L. G. Abele and D. L. Felder for specimens; M. Schuh, G. Bürkle, D. Horst, J. A. Cuesta, J. Christy, DBML, STRI and INRENA for support during collections; M. Frye, S. Kumar, and I. Ruvinsky for methodological advice; S. Kumar for the program PHYLTEST; E. Geißler and A. Beausang for help with figures; and C. A. Hass, S. Kumar, J. Reimer, and Cl. Schubart for comments on the manuscript. This project was funded by the DFG (C.D.S. and R.D.) and NSF (S.B.H.).

Correspondence and requests for materials should be addressed to C.D.S. (e-mail: cds5356@usl.edu).

The biosynthetic pathway of vitamin C in higher plants

Glen L. Wheeler, Mark A. Jones & Nicholas Smirnoff

School of Biological Sciences, University of Exeter, Hatherly Laboratories, Prince of Wales Road, Exeter EX4 4PS, UK

Vitamin C (L-ascorbic acid) has important antioxidant and metabolic functions in both plants and animals, but humans, and a few other animal species, have lost the capacity to synthesize it¹. Plant-derived ascorbate is thus the major source of vitamin C in the human diet. Although the biosynthetic pathway of L-ascorbic acid in animals is well understood², the plant pathway has remained unknown³—one of the few primary plant metabolic pathways for which this is the case. L-ascorbate is abundant in plants (found at concentrations of 1–5 mM in leaves and 25 mM in chloroplasts^{3,4}) and may have roles in photosynthesis and transmembrane electron transport^{3–5}. We found that D-mannose and L-galactose are efficient precursors for ascorbate synthesis and are interconverted by GDP-D-mannose-3,5-epimerase. We have identified an enzyme in pea and *Arabidopsis thaliana*, L-galactose dehydrogenase, that catalyses oxidation of L-galactose to L-galactono-1,4-lactone. We propose an ascorbate biosynthesis pathway involving GDP-D-mannose, GDP-L-galactose, L-galactose and L-galactono-1,4-lactone, and have synthesized ascorbate from GDP-D-mannose by way of these intermediates *in vitro*. The definition of this biosynthetic pathway should allow engineering of plants for increased ascorbate production, thus increasing their nutritional value and stress tolerance.

Evidence for the ascorbate-biosynthesis pathways so far proposed for plants is inconclusive. The most effective exogenous precursor of L-ascorbic acid is L-galactono-1,4-lactone, which is converted directly to ascorbate by a mitochondrial enzyme, L-galactono-1,4-lactone dehydrogenase^{6,7}. However, the role of L-galactono-1,4-lactone as a physiological precursor has been disputed⁸. L-galactono-1,4-lactone has not been detected in plants and, more significantly, its proposed production by D-galacturonic acid⁹ requires inversion of the hexose carbon skeleton, which extensive radiolabel tracer studies have shown does not occur during ascorbate synthesis from glucose¹⁰. An alternative pathway, involving the unusual intermediates D-glucosone and L-sorbose, has been suggested¹¹; this pathway involves no inversion of the carbon chain. However, the evidence that the physiological precursors are osones is also not conclusive.

If plants could produce L-galactono-1,4-lactone without inversion of the carbon chain, evidence for its involvement in ascorbate biosynthesis would be more powerful. To investigate the possible source of L-galactono-1,4-lactone in plants, we supplied L-galactose to barley leaf slices. This resulted in a rapid and substantial increase in the foliar ascorbate concentration, similar to that induced by L-

galactono-1,4-lactone (Fig. 1a). Feeding with L-galactose also increased ascorbate concentration in *A. thaliana* leaves and embryonic axes of germinating pea seedlings. The identity of the product as L-ascorbate was confirmed by its reactivity with ascorbate oxidase, by its ability to reduce acidic dichlorophenolindophenol (DCPIP), and by co-chromatography with L-ascorbate using thin-layer chromatography (TLC) and high-performance liquid chromatography (HPLC). Exogenous L-galactose accumulated in pea embryonic axes. The L-galactose was undetectable by gas chromatography (GC) 1 h after removal of the external supply, showing that it is rapidly and efficiently metabolized.

L-galactose is therefore an effective precursor of L-ascorbate in plants. Oxidation of L-galactose at position C1 would result in the production of L-galactono-1,4-lactone. An enzyme catalyzing this reaction was detected in cell-free extracts of *A. thaliana* leaves and pea embryonic axes. Both of these extracts supported L-galactose-dependent reduction of NAD⁺. The enzyme activity from pea embryonic axes was partially purified. The reduction activity with NADP⁺ was 10% of that with NAD⁺. The enzyme exhibited no

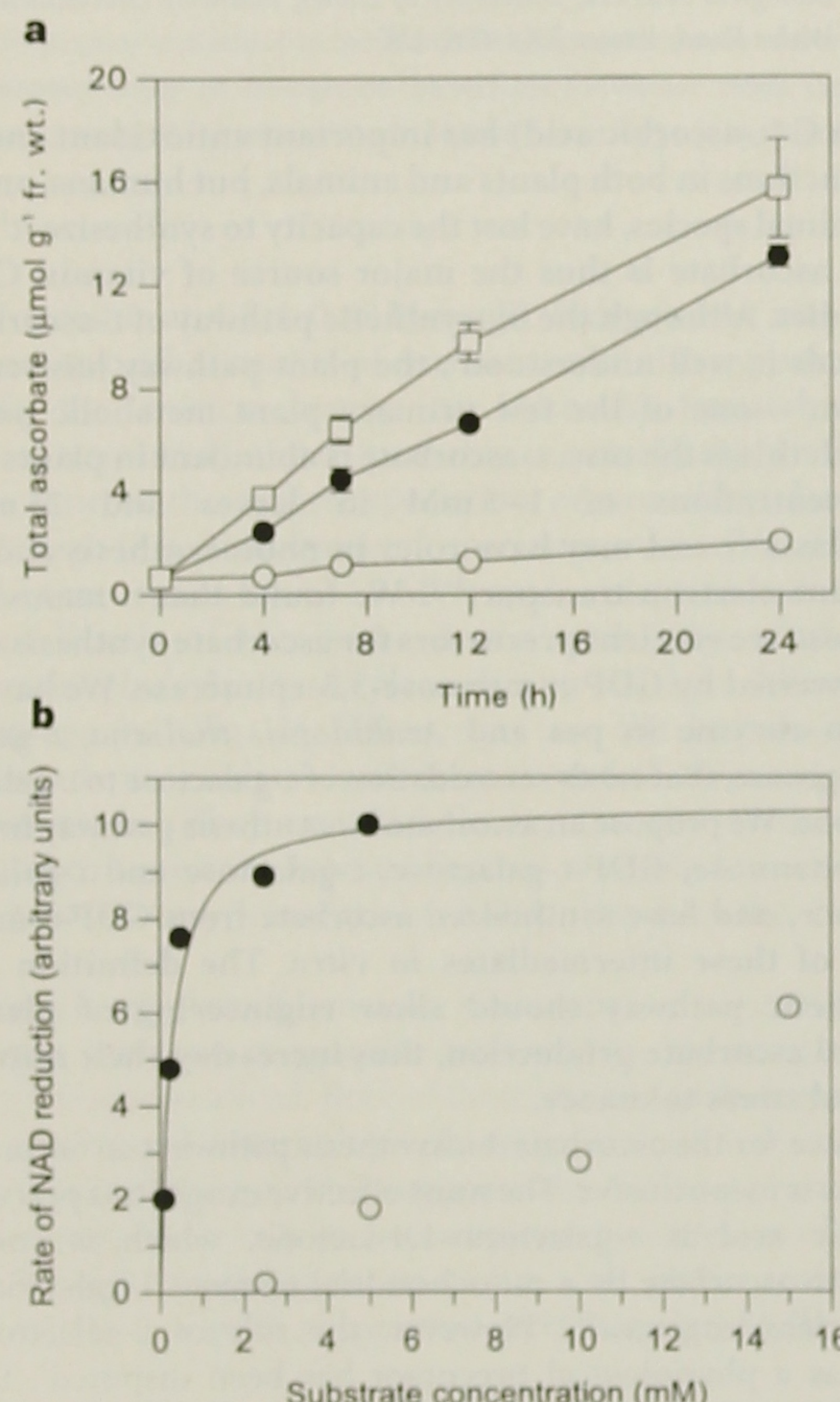


Figure 1 L-galactose is converted to L-ascorbate via L-galactono-1,4-lactone using L-galactose dehydrogenase. **a**, Ascorbate accumulation in barley leaves supplied with potential ascorbate precursors. Leaf segments were floated on water (open circles), 25 mM L-galactose (filled circles) or 25 mM L-galactono-1,4-lactone (open squares) in the light. The error bars indicate standard errors ($n = 3$). **b**, Identification of L-galactose dehydrogenase from pea embryonic axes. Activity was detected as L-galactose-dependent reduction of NAD⁺ and the reaction product was L-galactono-1,4-lactone (filled circles). The K_m for L-galactose was 0.3 mM and the pH optimum was pH 7.5–8.0. L-sorbose was oxidized with low affinity (open circles) and this oxidation activity co-purified with L-galactose dehydrogenase.

Table 1 Comparison of the metabolism of D-[U-¹⁴C]glucose and D-[U-¹⁴C]mannose by *A. thaliana* leaves

	¹⁴ C-glucose	¹⁴ C-mannose
Percentage of total ¹⁴ C		
Insoluble	50.1 ± 3.5	29.2 ± 2.8
Soluble	45.9 ± 2.9	67.9 ± 2.9
CO ₂	4.0 ± 1.0	2.9 ± 0.8
Ascorbic acid	1.0 ± 0.2	10.0 ± 1.2
Percentage of soluble ¹⁴ C		
Basic fraction	12.4 ± 5.8	4.1 ± 0.6
Neutral fraction	33.6 ± 5.8	62.7 ± 22.1
Acidic fraction		
60 mM formic acid eluent	11.2 ± 0.6	12.8 ± 2.3
2 M formic acid eluent	25.9 ± 5.1	19.5 ± 1.4

The leaves were fed labelled compounds through their petioles and incubated for 4 h in the light. ¹⁴CO₂ was trapped and the leaves extracted in 5% perchloric acid. The extract was neutralized and soluble components separated by ion-exchange chromatography into neutral, basic, and two acidic fractions. These two acidic fractions were eluted with 60 mM and 2 M formic acid. Ascorbic acid elutes in the 60 mM fraction. Values are means ± standard error ($n = 3$).

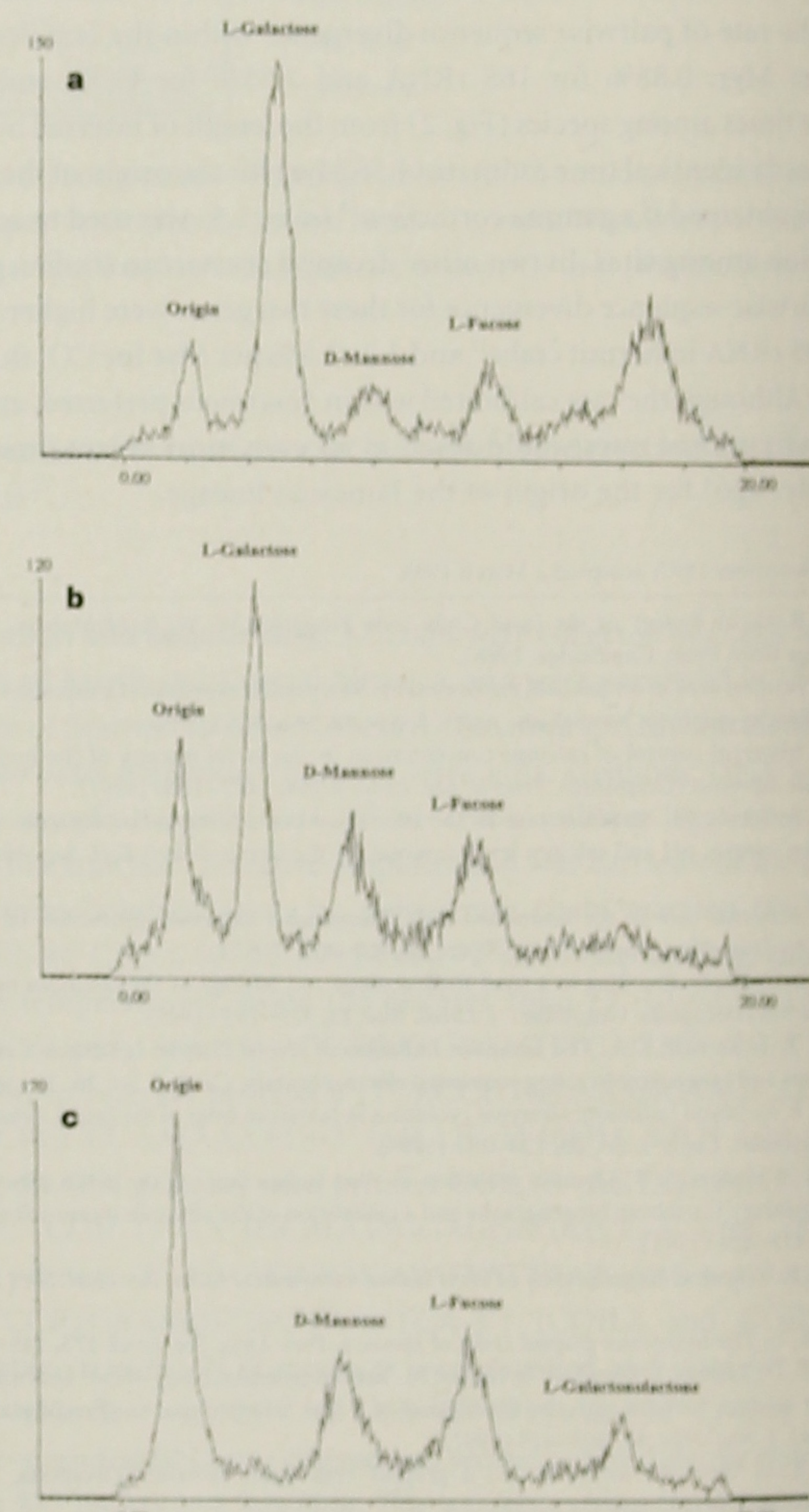


Figure 2 *In vitro* conversion of GDP-D-mannose to L-galactose and L-galactono-1,4-lactone by pea embryonic axis extracts. Crude extracts were incubated with GDP-D-[U-¹⁴C]mannose. After incubation, the reaction products were separated into neutral (free sugars) and acidic (phosphorylated or GDP-sugars) fractions by anion-exchange chromatography. The acidic fraction was then hydrolysed with trifluoroacetic acid to release free sugars. Sugars from both fractions were then separated by TLC and ¹⁴C label was detected by scanning the plates. **a**, TLC separation of sugars from acidic reaction products after 4 h incubation. Appearance of ¹⁴C in L-galactose shows the GDP-D-mannose was converted to GDP-L-galactose. GDP-L-fucose was also formed. **b**, Labelled L-galactose was detected in the neutral fraction of the reaction products, showing that free L-galactose was formed from GDP-D-mannose. **c**, Addition of 5 mM NAD⁺ for the final 3.5 h of the reaction shown in **b** resulted in disappearance of L-galactose and formation of L-galactono-1,4-lactone.

activity that was dependent on D-galactose, D-glucose, D-mannose, L-fucose and D-arabinose. The reaction product showed a positive response with the hydroxylamine assay for lactones, with 1:1 stoichiometry between NADH formation and lactone production (in L-galactono-1,4-lactone equivalents). We purified the reaction product and subjected it to GC-mass spectrometry (MS) to distinguish between two possible reaction products (C6 oxidation results in a uronic acid or lactone, whereas C1 oxidation results in an aldonic acid or lactone). We detected one peak, which co-chromatographed with authentic L-galactono-1,4-lactone. Its mass spectrum was identical to that of L-galactono-1,4-lactone. We assume that the initial product, from L-galactopyranose, was L-galactono-1,5-lactone which is relatively unstable and spontaneously converts to the 1,4 lactone. The K_m for L-galactose was 0.3 mM (Fig. 1b). The enzyme oxidized L-sorbosone, another suggested intermediate in plant ascorbate biosynthesis¹¹, but with very low affinity (Fig. 1b). This activity had a similar preference for NAD⁺. The product would be L-ascorbate acid¹², explaining the incorporation of labelled L-sorbosone into ascorbate¹¹. L-sorbosone has the same configuration as L-galactose at C4 and C5 and the chiral centre at C3 is lost in ascorbate.

We have therefore demonstrated the existence of a new higher-plant enzyme, L-galactose dehydrogenase (L-galactose:NADP⁺ oxidoreductase), which forms L-galactono-1,4-lactone from L-galactose with high affinity and specificity. Other dehydrogenases that oxidize C1 of non-phosphorylated aldoses have been identified, for example D-galactose dehydrogenase in *Pseudomonas fluorescens*¹³ L-fucose dehydrogenase in mammals¹⁴ and fungi¹⁵ and D-arabinose dehydrogenase in *Candida albicans*¹⁶. The latter enzyme has been implicated in synthesis of D-arabino-1,4-lactone, which is the precursor of D-erythroascorbate, the yeast analogue of L-ascorbate¹⁶.

L-galactose constitutes a small proportion of the galactose in non-cellulosic cell-wall polymers^{17,18}. L-galactose residues in the cell wall are derived from GDP-L-galactose, which is formed by GDP-D-mannose-3,5-epimerase, a poorly characterized enzyme reported in *Chlorella* and flax seeds^{19–21}. We have detected GDP-mannose-3,5-

epimerase activity in extracts of pea embryonic axes (Fig. 2a) and in ammonium-sulphate precipitates from *A. thaliana* leaves, using GDP-D-[U-¹⁴C]mannose (universally labelled GDP-D-mannose) as substrate. The products were free L-galactose and one or more acidic compounds, which produced L-galactose after hydrolysis. These acidic compounds must be GDP-L-galactose and/or L-galactose-1-phosphate (Fig. 2a, b). We confirmed the identity of the non-acidic product as L-galactose, rather than D-galactose, by its lack of reactivity with D-galactose dehydrogenase²². L-galactose is formed by hydrolysis of GDP-L-galactose; we do not yet know if L-galactose-1-phosphate is an intermediate. We suggest that formation of L-galactose resulted from a specific hydrolytic activity, because very little free mannose was released from GDP-mannose (Fig. 2b).

NAD⁺ added to the reaction mixture during the latter part of the incubation period resulted in loss of L-galactose from the neutral sugar fraction and appearance of radioactivity in a compound with the same mobility as L-galactono-1,4-lactone (Fig. 2c). Therefore, to confirm that L-galactono-1,4-lactone was produced from GDP-mannose, we prepared a pea embryonic axis extract containing intact mitochondria. Assays were carried out as above but with the addition of cytochrome c (1.5 mg ml⁻¹) as an electron acceptor for L-galactono-1,4-lactone dehydrogenase^{6,7}. We added unlabelled carrier ascorbate to the reaction mixture and then separated ascorbate by ion-exchange chromatography followed by TLC or HPLC. A radioactive peak that co-chromatographed with carrier L-ascorbate was detected in both systems. Treatment with ascorbate oxidase removed the radiolabelled HPLC peak. This clearly shows the ability of the tissue extract to produce ascorbate from GDP-D-mannose.

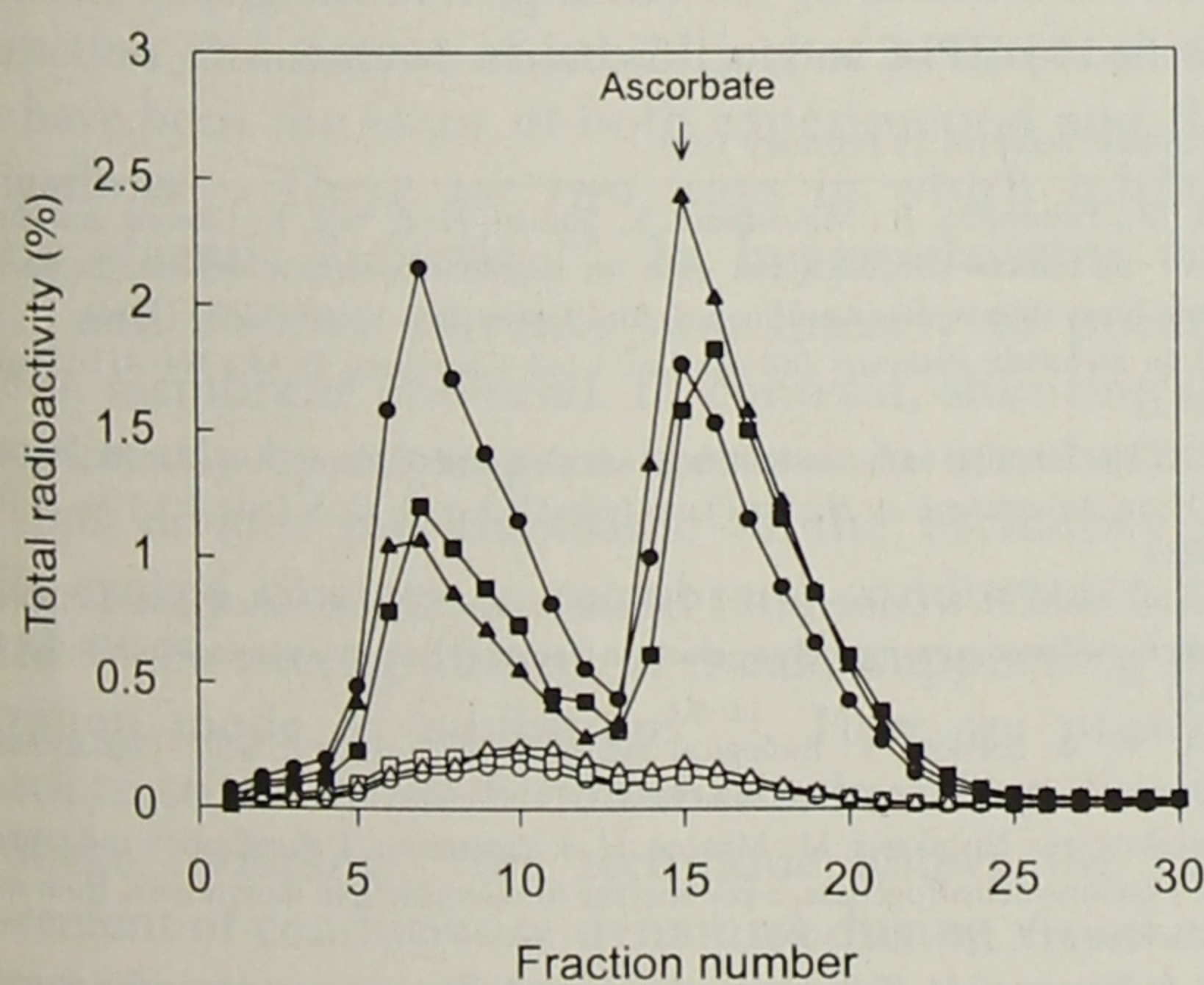


Figure 3 Comparison of the incorporation of D-[U-¹⁴C]glucose (open symbols) and D-[U-¹⁴C]mannose (closed symbols) into ascorbate by *A. thaliana* leaves. The leaves were fed labelled compounds through their petioles, incubated for 4 h in the light, and then extracted and fractionated as described in Table 1. The ¹⁴C content of ascorbic acid was determined after separation of the 60 mM formic acid fraction by HPLC, with correction for ascorbate loss during processing. The radioactive peak preceding ascorbate in the HPLC trace is largely dehydroascorbate.

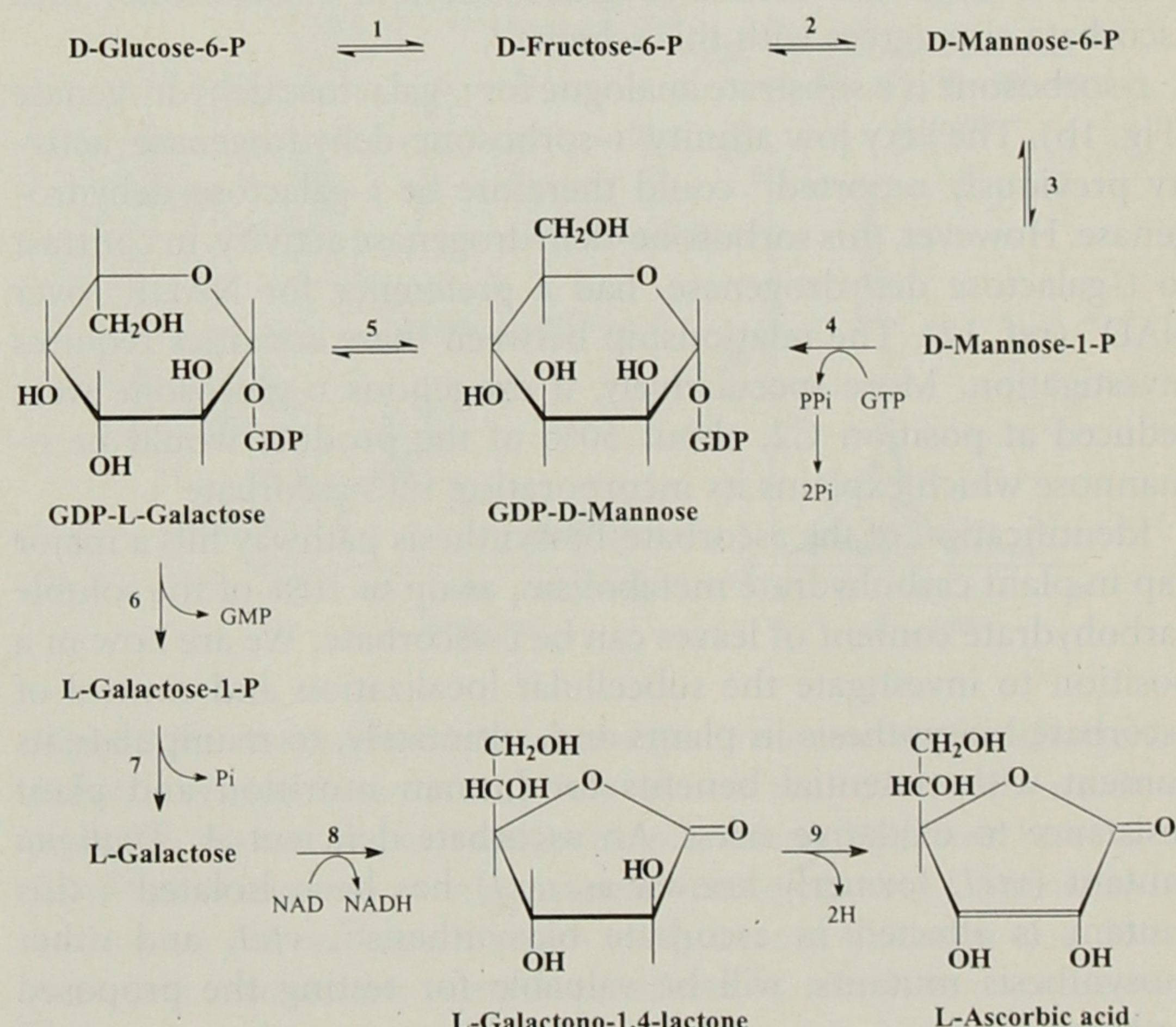


Figure 4 A proposed pathway for the biosynthesis of L-ascorbic acid in plants. The enzymes 1–5, which convert D-glucose-6-phosphate (D-glucose-6-P) to GDP-D-mannose and GDP-L-galactose, have been previously identified and provide GDP-sugar precursors for polysaccharide synthesis. L-galactose, the first dedicated intermediate, is provided by hydrolysis of GDP-L-galactose; a two-step hydrolysis (steps 6 and 7) through L-galactose-1-phosphate is shown, although this is speculative. L-galactose is oxidized at position C1 by L-galactose dehydrogenase (step 8, L-galactose:NAD⁺ oxidoreductase), forming L-galactono-1,4-lactone. This is oxidized by mitochondrial L-galactono-1,4-dehydrogenase (step 9) to L-ascorbic acid. Enzymes: 1, hexose phosphate isomerase; 2, phosphomannose isomerase; 3, phosphomannose mutase; 4, GDP-D-mannose pyrophosphorylase; 5, GDP-D-mannose-3,5-epimerase; 8, L-galactose dehydrogenase; 9, L-galactono-1,4-lactone dehydrogenase.

D-mannose is not extensively metabolized through glycolysis in plants and is instead mainly used in production of nucleotide sugar intermediates which are precursors for polysaccharides and glycoproteins¹⁷. Exogenous mannose is readily phosphorylated to mannose-6-phosphate^{17,23}. To confirm that the proposed biosynthetic pathway occurs *in vivo*, we fed D-[U-¹⁴C]mannose to *A. thaliana* leaves and compared its incorporation into ascorbate with incorporation of D-[U-¹⁴C]glucose (Fig. 3, Table 1). In agreement with earlier reports^{10,11,24}, 1% of the labelled glucose was converted to ascorbate. In contrast, 10% of the labelled mannose was incorporated into ascorbate, showing that this is a major metabolic fate for this sugar. The same result was found with marrow (*Cucurbita pepo*) roots. High concentrations of exogenous mannose did not affect ascorbate pool size, indicating that its conversion to L-galactose may be more rate-limiting than oxidation of L-galactose and L-galactono-1,4-lactone to produce ascorbate.

These results allow us to propose a pathway for ascorbate biosynthesis in higher plants that is consistent with earlier evidence (Fig. 4). We have demonstrated the ability of plant extracts to catalyse all the proposed reactions, including L-galactose oxidation by L-galactose dehydrogenase, a new enzyme in higher plants. The pathway reconciles the apparent contradiction between the ease of oxidation of L-galactono-1,4-lactone to ascorbate and earlier radiolabelling data. Pioneering work showed that, during conversion of D-glucose to ascorbate in plants, there is conservation of the hydroxymethyl group at C6, an epimerization at C5 and no inversion of the carbon chain^{8,10,11}. Our pathway, in which L-galactono-1,4-lactone is produced from D-glucose and D-mannose through GDP-D-mannose and L-galactose, is consistent with these requirements. We suggest that the ability of plants to incorporate radiolabel from the osones (D-glucosone and L-sorbosone) into ascorbate also agrees with this scheme¹¹.

L-sorbosone is a substrate analogue for L-galactose dehydrogenase (Fig. 1b). The very low affinity 'L-sorbosone-dehydrogenase' activity previously reported¹² could therefore be L-galactose dehydrogenase. However, this sorbosone-dehydrogenase activity, in contrast to L-galactose dehydrogenase, had a preference for NADP⁺ over NAD⁺ (ref. 12). The relationship between these activities requires investigation. More speculatively, if exogenous D-glucosone were reduced at position C2, about 50% of the product would be D-mannose which explains its incorporation into ascorbate¹¹.

Identification of the ascorbate-biosynthesis pathway fills a major gap in plant carbohydrate metabolism, as up to 10% of the soluble carbohydrate content of leaves can be L-ascorbate. We are now in a position to investigate the subcellular localization and control of ascorbate biosynthesis in plants and, ultimately, to manipulate its content with potential benefits for human nutrition and plant resistance to oxidative stress. An ascorbate-deficient *A. Thaliana* mutant (*vtc1*, formerly known as *soz1*) has been isolated²⁴; this mutant is affected in ascorbate biosynthesis²⁵. *vtc1*, and other biosynthesis mutants, will be valuable for testing the proposed pathway. □

Methods

Plant material. Primary leaves of 1-week-old barley (*Hordeum vulgare* cv Golden Promise) seedlings, *Arabidopsis thaliana* (Col-0) leaves and embryonic axes dissected from pea (*Pisum sativum* cv Meteor) seedlings 24 h after imbibition were used.

Identification of ascorbate as the *in vivo* product of L-galactose metabolism. Tissue was extracted, and ascorbate analysed, by ascorbate oxidase²⁵. Identity of ascorbate was confirmed by TLC combined with DCPIP staining²⁶ and HPLC²⁵.

L-galactose dehydrogenase activity. Tissue was homogenized in 50 mM Tris-HCl pH 7.5 containing 20% (v/v) glycerol, 1 mM EDTA and 2 mM dithiothreitol (DTT). Enzyme activity precipitating at between 50% and 75% ammonium sulphate saturation was further purified by hydrophobic interaction chromatography (phenyl sepharose). We assayed enzyme activity by

following NAD(P)H formation at 340 nm in 50 mM tris-HCl buffer, pH 7.5, with 0.1 mM NAD(P)⁺ and several concentrations of L-galactose. The identity of the reaction product was determined by a lactone assay¹⁶ and GC-MS. Before GC analysis, the product was delactonized by incubation for 2 h at pH 9.5 and was passed through a Dowex 1-formate column. After a water wash, the column was eluted with 0.1 M formic acid. The eluate was brought to 1 M formic acid and evaporated under an air stream to relactonize the product. The product was then dissolved in pyridine, derivatized with trimethylsilylimidazole with and without methoxyamine²⁷, and analysed by GC (Hewlett Packard Ultra 2 capillary column) and GC-MS (Hewlett Packard Ultra 1 capillary column coupled to a Hewlett Packard 5970 mass selective detector).

GDP-D-mannose-3,5-epimerase activity. Tissue (0.35 g fresh weight per ml) was homogenized in 100 mM tris-HCl buffer pH 7.6 containing 5 mM DTT, 1 mM EDTA and 1% polyvinylpolypyrrolidone before centrifugation at 12,000 g for 20 min. Extracts containing intact mitochondria were prepared by including 0.33 M sorbitol in the extraction medium as an osmoticum. The supernatant was then either used directly as a crude extract or precipitated with 90% saturation ammonium sulphate, and was then desalting with Sephadex G-25 (Pharmacia PD10 column). Crude extracts or precipitates (30 µl) were incubated with 3.7 kBq GDP-D-[U-¹⁴C]mannose (Amersham, UK) for measurement of ascorbate synthesis in 70 µl 25 mM Tris-HCl pH 8.0 containing 2 mM EDTA at 25 °C. The reaction products were passed through a SAX anion-exchange column (HPLC Technology, Macclesfield, UK). Neutral fractions were deionized with an SCX cation-exchange column (HPLC Technology, Macclesfield, UK) before TLC. GDP-sugars and sugar phosphates were eluted from the SAX column with 2 M formic acid and the free sugars were released by hydrolysis with 2 M trifluoroacetic acid at 80 °C for 1 h before TLC. Sugars were separated by TLC on silica plates (Whatman) impregnated with 0.3 M sodium dihydrogen orthophosphate, using an acetone/butanol/water (8:1:1 by volume) solvent²⁸. TLC plates were scanned with a Berthold Linear Analyser to detect radioactivity. Radioactive peaks were identified by co-chromatography with sugar standards detected by aniline/diphenylamine stain²⁹ and lactones by hydroxylamine/FeCl₃ (ref. 29). D- and L-galactose are not resolved, so the identity of the reaction product was confirmed by using D-galactose dehydrogenase to selectively remove this compound²².

[U-¹⁴C]glucose and [U-¹⁴C]mannose metabolism. Labelled compounds (Amersham, UK) were fed to cut leaves through the transpiration stream²⁵. The extracts were fractionated by ion-exchange chromatography. Ascorbate was further purified by HPLC and its ¹⁴C content determined²⁵.

Received 12 January; accepted 19 February 1998.

- Nishikimi, M., Fukuyama, R., Minoshima, S., Simizu, N. & Yagi, K. Cloning and chromosomal mapping of the human nonfunctional gene for L-gulono-γ-lactone oxidase, the enzyme for L-ascorbic acid biosynthesis missing in man. *J. Biol. Chem.* **269**, 13685–13688 (1994).
- Burns, J. J. in *Metabolic Pathways* 2nd edn Vol. 1 (ed. Greenberg, D. M.) 394–411 (Academic, New York, 1967).
- Smirnoff, N. The function and metabolism of ascorbic acid in plants. *Ann. Bot.* **78**, 661–669 (1996).
- Foyer, C. H. in *Antioxidants in Higher Plants* (eds Alscher, R. G. & Hess, J. L.) 31–58 (CRC, Boca Raton, 1993).
- Horemans, N., Asard, H. & Caubergs, R. J. The role of ascorbate free radical as an electron acceptor to cytochrome b-mediated transmembrane electron transport in higher plants. *Plant Physiol.* **104**, 1435–1458 (1994).
- Mapson, L. W. & Breslow, E. Biological synthesis of L-ascorbic acid: L-galactono-γ-lactone dehydrogenase. *Biochem. J.* **68**, 395–406 (1958).
- Oba, K., Ishikawa, S., Nishikawa, M., Mizuno, H. & Yamamoto, T. Purification and properties of L-galactono-γ-lactone dehydrogenase, a key enzyme for ascorbic acid biosynthesis, from sweet potato roots. *J. Biochem.* **117**, 120–124 (1995).
- Loewus, F. A. & Loewus, M. B. Biosynthesis and metabolism of L-ascorbic acid in plants. *Crit. Rev. Plant Sci.* **5**, 101–119 (1987).
- Mapson, L. W. & Isherwood, F. A. Biological synthesis of L-ascorbic acid: the conversion of derivatives of D-galacturonic acid to L-ascorbate in plant extracts. *Biochem. J.* **64**, 13–22 (1956).
- Loewus, F. A. Tracer studies of ascorbic acid formation in plants. *Phytochemistry* **2**, 109–128 (1963).
- Saito, K., Nick, J. A. & Loewus, F. A. D-Glucosone and L-sorbosone, putative intermediates of L-ascorbic acid biosynthesis in detected bean and spinach leaves. *Plant Physiol.* **94**, 1496–1500 (1990).
- Loewus, M. W., Bedgar, D. L., Saito, K. & Loewus, F. A. Conversion of L-sorbosone to L-ascorbic acid by a NADP⁺-dependent dehydrogenase in bean and spinach leaf. *Plant Physiol.* **94**, 1492–1495 (1990).
- Maier, E. & Kurtz, G. D-galactose dehydrogenase from *Pseudomonas fluorescens*. *Meth. Enzymol.* **89**, 176–181 (1982).
- Schachter, H., Sarney, J., McGuire, E. J. & Roseman, S. Isolation of diposphopyridine nucleotide-dependent L-fucose dehydrogenase from pork liver. *J. Biol. Chem.* **244**, 4785–4792 (1969).
- Conter, P. F., Guimarães, M. F. & Veiga, L. A. Induction and repression of L-fucose dehydrogenase of *Pullularia pullulans*. *Can. J. Microbiol.* **30**, 753–757 (1984).
- Kim, S.-T., Huh, W.-K., Kim, J.-Y., Hwang, S.-W. & Kang, S.-O. D-Arabinose dehydrogenase and biosynthesis of erythroascorbate in *Candida albicans*. *Biochim. Biophys. Acta* **1297**, 1–8 (1996).
- Roberts, R. M. The metabolism of D-mannose-¹⁴C to polysaccharide in corn roots. Specific labelling of L-galactose, D-mannose, and L-fucose. *Arch. Biochem. Biophys.* **145**, 685–692 (1971).
- Baydoun, E. A.-H. & Fry, S. C. [2-³H]Mannose incorporation in cultured plant cells: investigation of L-galactose residues of the primary wall. *J. Plant Physiol.* **132**, 484–490 (1988).

19. Barber, G. A. Observations on the mechanisms of the reversible epimerization of GDP-D-mannose to GDP-L-galactose by an enzyme from *Chlorella pyrenoidosa*. *J. Biol. Chem.* **254**, 7600–7603 (1979).
20. Barber, G. A. Synthesis of L-galactose by plant enzyme systems. *Arch. Biochem. Biophys.* **147**, 619–623 (1971).
21. Feingold, D. S. in *Encyclopedia of Plant Physiology*, Vol. 13A (eds Loewus, F. A. & Tanner, W.) 3–76 (Springer, Berlin, 1982).
22. Roberts, R. M. & Harrer, E. Determination of L-galactose in polysaccharide material. *Phytochemistry* **12**, 2679–2682 (1973).
23. Harris, G. C. et al. Mannose metabolism in corn and its impact on leaf metabolites, photosynthetic gas exchange, and chlorophyll fluorescence. *Plant Physiol.* **82**, 1081–1089 (1986).
24. Conklin, P. L., Williams, E. H. & Last, R. L. Environmental stress sensitivity of an ascorbic acid-deficient *Arabidopsis* mutant. *Proc. Natl Acad. Sci. USA* **93**, 9970–9974 (1996).
25. Conklin, P. L., Pallanca, J. E., Last, R. L. & Smirnoff, N. L-Ascorbic acid metabolism in the ascorbate-deficient *Arabidopsis* mutant *vtc1*. *Plant Physiol.* **115**, 1277–1285 (1997).
26. Chen, Y.-T., Isherwood, F. A. & Mapson, L. W. Quantitative estimation of ascorbic acid and related substances in biological extracts by separation on a paper chromatogram. *Biochem. J.* **55**, 821–823 (1953).
27. Andrews, M. A. Capillary gas-chromatographic analysis of monosaccharides: improvements and comparisons using trifluoroacetylation and trimethylsilylation of sugar O-benzyl and O-methyl oximes. *Carbohydrate Res.* **194**, 1–19 (1989).
28. Ghebragabher, M., Ruffini, S., Monaldi, B. & Lato, M. Thin layer chromatography of monosaccharides. *J. Chromatogr.* **127**, 133–162 (1976).
29. Dawson, R. M. C., Elliott, D. C., Elliott, W. H. & Jones, K. M. (eds) *Data for Biochemical Research* 2nd edn. (Clarendon, Oxford, 1969).

Acknowledgements. The research was supported by a BBSRC studentship (G.L.W.), a Nuffield Student Bursary (M.A.J.) and Zeneca Agrochemicals. We thank Nippon-Roche for the gift of L-sorbose. Earlier work by J. Pallanca, funded by the BBSRC BOMRIP programme, provided a basis for this research. We thank M. Raymond for technical assistance; J. Kingdon and J. Hindley for growing the plants; and W. Schuch for his support.

Correspondence and requests for materials should be addressed to N.S. (e-mail: N.Smirnoff@exeter.ac.uk).

Visual input evokes transient and strong shunting inhibition in visual cortical neurons

Lyle J. Borg-Graham, Cyril Monier & Yves Frégnac

Equipe Cognosciences, Institut Alfred Fessard, CNRS, Avenue de la Terrasse, 91198 Gif sur Yvette, France

The function and nature of inhibition of neurons in the visual cortex have been the focus of both experimental and theoretical investigations^{1–7}. There are two ways in which inhibition can suppress synaptic excitation^{2,8}. In hyperpolarizing inhibition, negative and positive currents sum linearly to produce a net change in membrane potential. In contrast, shunting inhibition acts nonlinearly by causing an increase in membrane conductance; this divides the amplitude of the excitatory response. Visually evoked changes in membrane conductance have been reported to be nonsignificant or weak, supporting the hyperpolarization mode of inhibition^{3,9–12}. Here we present a new approach to studying inhibition that is based on *in vivo* whole-cell voltage clamping. This technique allows the continuous measurement of conductance dynamics during visual activation. We show, in neurons of cat primary visual cortex, that the response to optimally orientated flashed bars can increase the somatic input conductance to more than three times that of the resting state. The short latency of the visually evoked peak of conductance, and its apparent reversal potential suggest a dominant contribution from γ -aminobutyric acid ($(\text{GABA})_A$) receptor-mediated synapses. We propose that nonlinear shunting inhibition may act during the initial stage of visual cortical processing, setting the balance between opponent ‘On’ and ‘Off’ responses in different locations of the visual receptive field.

In the visual cortex, there are two major types of receptive fields, ‘simple’ and ‘complex’, based partly on the degree of spatial overlap between On and Off responses (evoked by an increase or decrease in light contrast, respectively) in the visual field^{4,13}. Simple receptive fields have distinct On and Off subfields, whereas these are over-

lapping in complex cells. We can consider how intracortical inhibition works during visual cortical processing at different levels. At the functional level, inhibition could help in the push–pull organization of opponent responses (for example, hyperpolarization is evoked by a decrease in light contrast in the On subfield) seen in simple receptive fields⁴. It could also control the spatial tuning of On and Off excitation, as intracortical blockade of γ -aminobutyric acid ($(\text{GABA})_A$) receptors results in loss of segregation of On and Off excitatory responses in simple cells, whether measured extracellularly¹ or intracellularly¹⁴.

At the biophysical level, even if shunting inhibition does exist, there is still a quantitative issue concerning its functional importance. As the reversal potential for $(\text{GABA})_A$ -mediated channels, which are probably responsible for the shunt in membrane conductance, is near the resting potential, shunting inhibition must produce a large change in the postsynaptic conductance to significantly counteract excitation. Simulations show that this shunt should be visible as a 100–200% increase in the somatic input conductance, $G_{\text{in}}(t)$, relative to the no-stimulus condition (characterized as G_{rest})^{2,15}. However, measurements from current clamp recordings have indicated limited conductance changes (relative

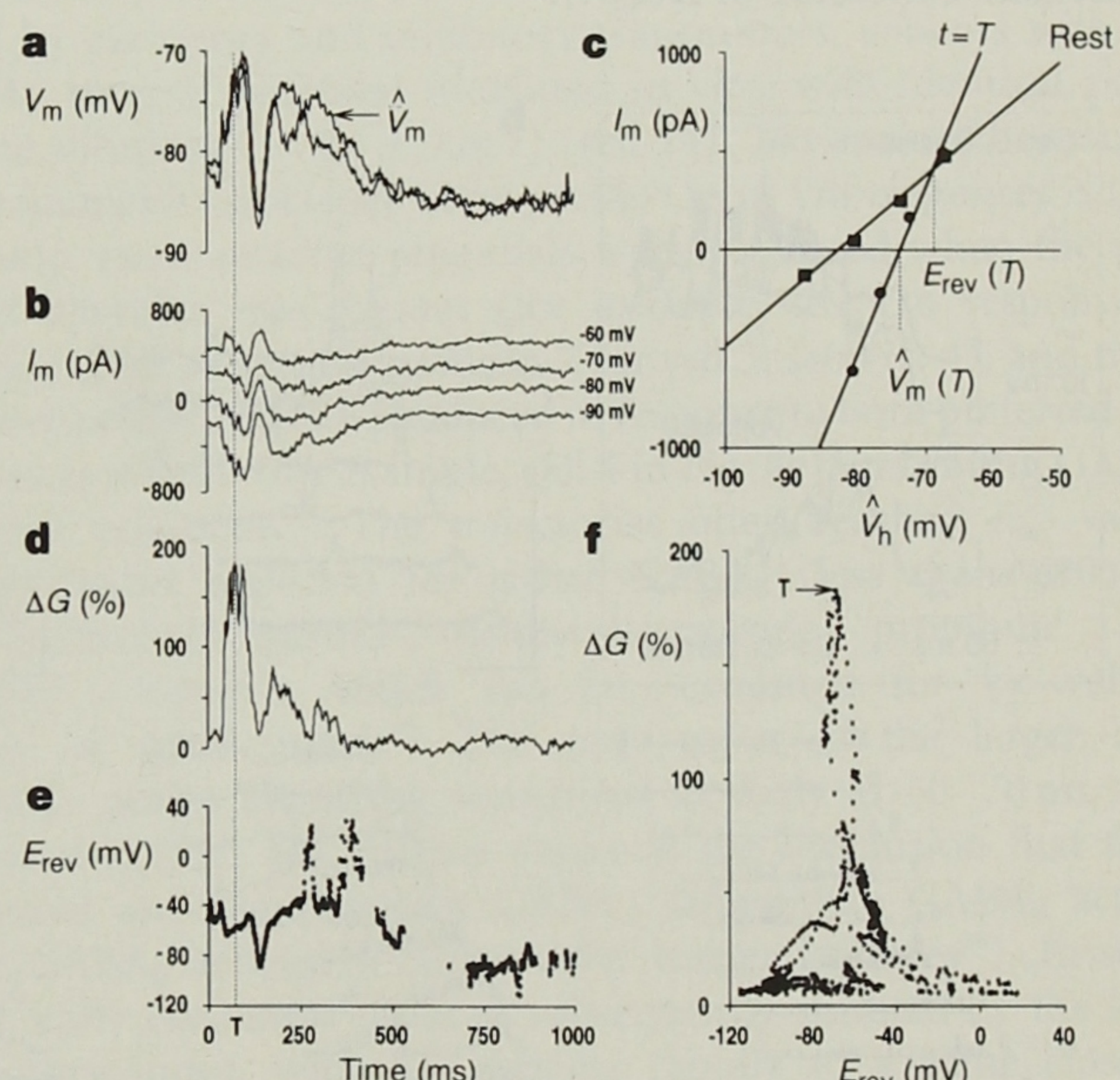


Figure 1 The visually evoked relative change in input conductance $\Delta G_{\text{in}}(t)$ and its apparent reversal potential $E_{\text{rev}}(t)$ are derived from the current waveforms measured by two to four voltage-clamp protocols, illustrated here for the subthreshold response of an end-stopped simple cell to an Off transition of a flashing bar (full response is shown in Fig. 2e, cell 4, position 8). **a**, Voltage responses under current clamp and predicted \hat{V}_m (arrow) from voltage-clamp currents, assuming a linear model. **b**, Responses under voltage clamp for four command holding potentials. **c**, I/V characteristics derived from linear regressions corresponding to the resting state (squares), the slope of which gives G_{rest} , and during visual activation (circles) at the time T marked by a dotted line in (a–e). The voltage axis, \hat{V}_m , corresponds to the command holding potential corrected for R_s . The interpolated voltage at zero current of the I/V characteristic at any given time predicts the current clamp response ($\hat{V}_m(t)$) in **c**. The stability of the recording, and the justification of a linear approximation for this subthreshold example, are shown by the close match between the original and the interpolated traces superimposed in **a**. **d**, Relative $\Delta G_{\text{in}}(t)$, derived continuously over the complete duration of the visual stimulation. **e**, $E_{\text{rev}}(t)$. **f**, Phase plot of relative $\Delta G_{\text{in}}(t)$ versus $E_{\text{rev}}(t)$, where each point represents averages taken over 1 ms, illustrating the various trajectories in time (arrow for time T). In this case, the conductance response at time 0 is $>105\%$ of the input conductance at rest because the tail of the On response starts 1000 ms earlier. All responses in this paper are averages of 10 trials.